

Thermal transitions and structural properties of synthetic cholesterol alkyl and alkenyl ethers: analogues of biological cholesterol esters¹

Richard J. Deckelbaum, Gidon Halperin, and David Atkinson

Departments of Gastroenterology and Pediatrics² and Lipid Research Laboratory, Department of Medicine B,³ Hadassah University Hospital, Jerusalem, Israel; Biophysics Institute, Boston University Medical Center, Boston, MA;⁴ and the Montreal Children's Hospital, Montreal, Canada²

Abstract Nine even-numbered saturated (C₄ to C₂₀) and two unsaturated (C_{18:1}, C_{18:2}) cholesterol alkyl ethers were studied by differential scanning calorimetry, polarizing microscopy, and X-ray powder diffraction. Seven of the nine saturated ethers examined melt into stable liquid crystal mesophases. Mesophase transition temperatures vary over a much narrower range than in cholesterol esters and are lower than those of corresponding esters. Polarizing microscopy and X-ray diffraction show structural similarities between cholesterol ethers and esters. Since cholesterol ethers behave similarly thermotropically to cholesterol esters, they may serve as suitable nonmetabolizable analogues for cholesterol esters in biological systems.—**Deckelbaum, R. J., G. Halperin, and D. Atkinson.** Thermal transitions and structural properties of synthetic cholesterol alkyl and alkenyl ethers: analogues of biological cholesterol esters. *J. Lipid Res.* 1983; **24**: 657–661.

Supplementary key words differential scanning calorimetry • X-ray diffraction

Synthetic cholesterol alkyl ethers have recently been utilized in studies following the uptake and degradation of plasma lipoprotein cholesterol in tissue culture and animal models (1, 2). Because these compounds are poorly catabolized by mammalian cells (3), they can serve as nonmetabolizable analogues in evaluating cholesterol ester uptake and distribution in cells.

This study examines the structural and thermal properties of straight chain saturated and two unsaturated ethers of cholesterol using differential scanning calorimetry, X-ray powder diffraction, and polarizing microscopy. Cholesterol ethers in general show lower melting temperatures from the crystalline state to the liquid than their ester counterparts and seven of the nine even-numbered saturated ethers studied (C₄ to C₂₀) have stable mesophases⁵ above the melting temperature of the crystal.

METHODS

Long chain unsaturated alcohols were obtained from Nu-Chek Prep, Inc. Other alcohols and *p*-toluenesulfonyl chloride were purchased from Sigma Chemical Co. After reaction, and extraction with hexane, cholesterol alkyl ethers were eluted from silicic acid columns in four successive chromatographies with increasing amounts of benzene relative to hexane, as previously described (4). Compounds were found to be greater than 99% pure by: *a*) thin-layer chromatography (petroleum ether–ether 98:2 and hexane–chloroform 7:3); *b*) gas–liquid chromatography showing a single elution peak only for each compound (3% QF-1 and 3% SE-30, Supelco, Inc.) (4); and *c*) differential scanning calorimetry (DSC) with sharp, single crystal melt transitions. The C₂₀ and C_{18:2} ethers, however, showed slightly wide and asymmetric crystal melting transitions by DSC, showing them not to be totally pure at the time of the experiments.

Differential scanning calorimetry

Samples (1–3 mg) of each ether were analyzed in a Perkin-Elmer DSC-2 differential scanning calorimeter. Samples in the crystalline state were sealed in aluminum pans, heated at 5°C/min to 20°C above the highest

Abbreviation: DSC, differential scanning calorimetry.

¹ Portions of this study were carried out during Dr. Deckelbaum's tenure as a Visiting Scientist at the McGill University-Montreal Children's Hospital Research Institute.

² R. J. Deckelbaum.

³ G. Halperin.

⁴ D. Atkinson.

⁵ The terms "mesophase" and "liquid crystal" refer to states of matter intermediate between the solid crystalline state, which possesses long-range positional and orientational order, and the isotropic liquid state, which has statistical long-range disorder.

melting transition, and then cooled to record the liquid crystalline transitions. Wherever possible, heating and cooling curves were obtained for mesomorphic transitions (smectic to cholesteric, cholesteric to isotropic), but in some cases recrystallization to the stable crystal form occurred before these liquid crystal transitions could be seen on heating. Heating and cooling rates were 5°C/min and full scale sensitivities varied from 1–5 mcal/sec for crystal melting transitions and 0.1–1 mcal/sec for liquid–crystal transitions. The transition temperatures were obtained by drawing a line through the steepest part of the leading edge of the transition peak to the extrapolated baseline and measuring the temperature at their intersection. Transition temperatures on three separate samples were repeatable to $\pm 0.5^\circ\text{C}$. Temperature calibration was performed within $\pm 0.2^\circ\text{C}$ using indium and cyclohexane standards. Enthalpies of transitions (ΔH) were calculated from the areas under peaks and related to the area of the crystal–liquid melting transition of indium standard. Enthalpies were determined on at least three separate samples for each ether and had a mean variation for duplicate determination of approximately 11% for crystalline melting transitions and 16% for mesophase transitions.

X-Ray diffraction

X-ray diffraction patterns of each ether were recorded using either a focusing camera with Elliot (5) toroidal mirror optics or a Luzatti-Baro camera modified to include a single focussing mirror. Nickel-filtered $\text{CuK}\alpha$ radiation from an Elliot GX-6 rotating anode generator or a Jarrel Ash microfocussing generator was used, respectively. Specimens were sealed in a 1-mm diameter Lindeman capillary tube and placed in a variable temperature sample holder.

Polarizing light microscopy

The nature of transitions recorded by DSC were confirmed using polarizing light microscopy. Samples of cholesterol ether were placed on a microscope slide, covered with a cover slip, and examined using a Zeiss standard NL polarizing light microscope with a controlled heating-cooling stage, at rates of 1–3°C/min. Changes of state (crystal, smectic, cholesteric, isotropic liquid) were identified by optical texture, signs of birefringence, and gross rheological changes,⁶ at temperatures matching transitions obtained on DSC (6).

⁶ Smectic and cholesteric refer to different liquid crystalline mesophases characteristic of cholesterol esters and, as found in this work, cholesterol ethers. In the smectic liquid crystalline state, planar arrays of molecules are regularly stacked with a periodicity of about 35 Å. This phase is characterized optically by uniaxial positive birefringence and by its "focal conic" structure under the polarizing microscope. In

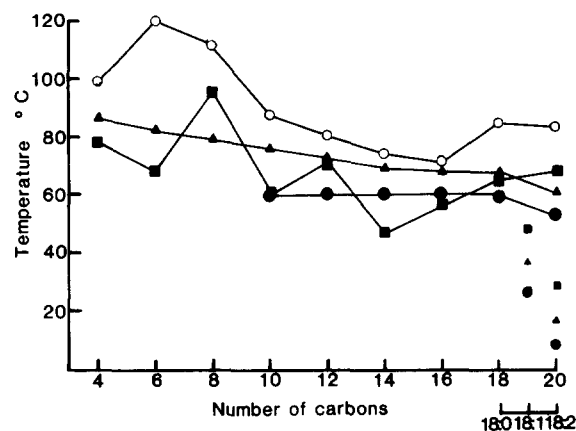


Fig. 1. Transition temperatures of cholesterol alkyl ethers: ■—■ crystal melting temperatures; ▲—▲ cholesteric to isotropic transitions; ●—● smectic to cholesteric transitions. Inset at lower right shows transition temperature for $\text{C}_{18:1}$ and $\text{C}_{18:2}$ unsaturated ethers. The crystal melting temperatures for corresponding cholesterol esters are shown for comparison (○—○).

RESULTS AND DISCUSSION

The thermodynamic data for even-numbered n-alkyl ethers from C_4 to C_{20} are given in Table 1. Fig. 1 records the crystal melting transition temperatures and the mesophase transition temperatures of the cholesterol ethers studied. In every case the crystalline melting temperature is below that of the analogous cholesterol ester. Unlike the esters, most (seven of nine) of the saturated ethers examined melt into a stable mesophase. The C_4 , C_6 , C_{10} , C_{12} , and C_{18} cholesterol ethers melt to cholesteric liquid crystals and C_{14} and C_{16} homologues melt to smectic mesophases. In the same series of cholesterol esters only C_4 , C_{10} , and C_{14} have mesophases above the crystal melt. Comparing cholesterol ether crystal melting temperatures to those of cholesterol esters, no consistent pattern is observed.

The liquid crystalline phase changes observed for the cholesterol ethers show relatively small differences in transition temperatures with increasing chain length of the ether. Between C_{10} to C_{18} , the smectic-cholesteric transition varies over only 2°C, and the cholesteric-isotropic 7°C. In every case, mesophase transitions occur at lower temperatures than those reported for cholesterol esters (7). Like the esters, the short chain cholesterol ethers, C_{4-8} exhibit cholesteric but no smectic mesophases (7).

Fig. 2 compares the crystalline melting transition enthalpies of cholesterol ethers to cholesterol esters. In

cholesteric liquid crystals, the molecules are ordered in helices about an axis at right angles to the long axis of the molecules, and the phase is characterized optically by a) circular dichroism, giving the phase its characteristic iridescent colors; b) negative birefringence; and c) high optical activity.

TABLE 1. Thermodynamic data for cholesterol alkyl ethers

Alkyl Ether	Transition	Transition Temperature	Transition Enthalpy	Transition Entropy
		°C	Kcal mol ⁻¹	cal mol ⁻¹ degree K ⁻¹
Butyrate (4:0)	Solid → cholesteric	78	5.89	16.78
	Cholesteric → isotropic	86.5	0.11	0.31
Caproate (6:0)	Solid → cholesteric	68	6.48	19.01
	Cholesteric → isotropic	81	0.17	0.47
Caprylate (8:0)	Solid → isotropic	95.5	7.22	19.58
	Cholesteric → isotropic	(79) ^a	0.20	0.57
Caprate (10:0)	Solid → cholesteric	60	5.25	15.75
	Smectic → cholesteric	(61)	0.20	0.59
	Cholesteric → isotropic	75.5	0.21	0.61
Laurate (12:0)	Solid → cholesteric	70.5	8.50	24.72
	Smectic → cholesteric	(61)	0.30	0.91
	Cholesteric → isotropic	72	0.29	0.85
Myristate (14:0)	Solid → smectic	47	10.53	32.90
	Smectic → cholesteric	60	0.45	1.36
	Cholesteric → isotropic	69.5	0.44	1.29
Palmitate (16:0)	Solid → smectic	56.5	13.62	41.34
	Smectic → cholesteric	60	0.54	1.62
	Cholesteric → isotropic	68	0.55	1.61
Stearate (18:0)	Solid → cholesteric	63.5	16.70	49.63
	Smectic → cholesteric	(59)	0.51	1.53
	Cholesteric → isotropic	68	0.66	1.94
Arachidate ^b (20:0)	Solid → isotropic	66.5	15.69	46.22
	Smectic → cholesteric	(52.5)	0.79	2.43
	Cholesteric → isotropic	(60.5)	0.73	2.20
Elaidate (18:1) (trans-9'-octadecenoyl)	Solid → isotropic	48	16.12	50.20
	Smectic → cholesteric	(26.5)	0.42	1.40
	Cholesteric → isotropic	(36.5)	0.32	1.02
Linoleate ^b (18:2) (cis,cis-9',12'-octadecadienyl)	Solid → isotropic	27.5	12.71	42.30
	Smectic → cholesteric	(8.5)	0.26	0.92
	Cholesteric → isotropic	(17.5)	0.17	0.57

^a Temperatures in parentheses are from cooling curves.

^b The C_{20:0} and C_{18:2} cholesterol ethers were seen to be not completely pure, both having slightly asymmetric and wide crystal melting transitions on DSC.

both ethers and esters, the C₄ to C₈ series and C₁₀ to C₁₈ series show linear increases in entropy suggesting a similar structural homologous series for separate groups in the crystalline form. In the cholesterol ether series, the ΔS of C₂₀ does not fall on the straight line for the C₁₀ to C₁₈ ethers. However, this probably reflects impurity since X-ray diffraction data (see below) are in keeping with homologous structure for the C₂₀ ether.

Mesophase transition entropies of cholesterol ethers are diagrammed in Fig. 3, and compared to cholesterol esters. Like the cholesterol esters, increasing chain length is associated with increasing entropy change. Introduction of double bands leads to lower entropy changes as shown in the insert to the figure. Entropy changes for all mesophase transitions are greater for cholesterol ethers, suggesting greater mesophase stability relative to cholesterol esters. Similarly, greater

temperature differences exist between smectic-cholesteric and cholesteric-isotropic transitions of cholesterol ethers relative to esters. Polarizing microscopy showed that optical properties of the mesophases of cholesterol ethers were identical to those of the cholesterol esters.

Fig. 4 shows the primary Bragg X-ray diffraction spacings in the low angle region of the diffraction pattern for the homologous series of cholesterol ethers (C₄ → C₂₀). Characteristic diffraction patterns for the C₁₈ and C₁₂ cholesterol ethers are illustrated in the insert.

These primary X-ray diffraction spacings suggest that the cholesterol ethers form at least two isostructural series C₁₄–C₂₀ and C₄–C₁₂. Similarities in the diffraction pattern and the diffraction spacing for the C₁₄–C₂₀ series suggest that the crystal packing of the cholesterol ethers in this series is of the “bimolecular layer” form

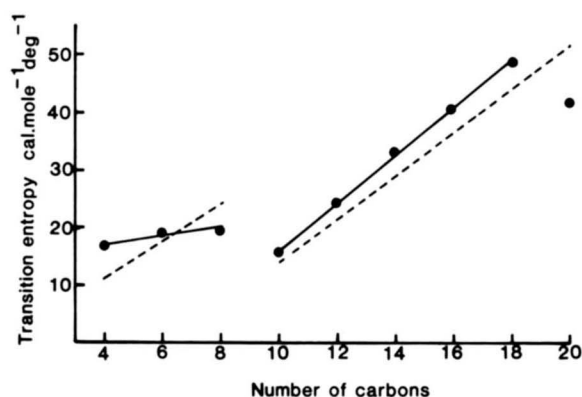


Fig. 2. Crystalline melting transition entropies of cholesterol alkyl ethers (●—●) and cholesterol esters (---○) of saturated fatty acids. Data for cholesterol esters are from reference 7.

described by Craven and DeTitta (8) for cholesteryl myristate. Single crystal studies have also demonstrated that the C_{14} – C_{18} cholesterol esters are isostructural with this packing. Craven and co-workers have similarly demonstrated that at least two different crystal packings are exhibited by the C_6 to C_{12} cholesterol esters. The crystal data for C_{10} and C_{12} (9) cholesterol esters demonstrate an identical molecular packing. C_6 cholesterol ester data suggest another molecular packing that is similar to that of cholesteryl oleate ($C_{18:1}$) (10, 11). Thus it seems probable by analogy that the cholesterol ethers in the C_4 – C_{12} series do not represent a single isostructural series and probably exhibit similar complexity in molecular packing to the cholesterol esters.

Like cholesterol esters, the cholesterol ethers show only one major diffraction spacing in the low angle re-

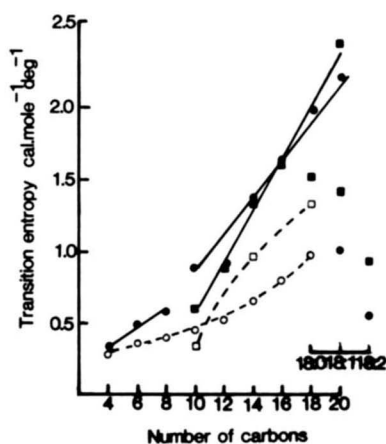


Fig. 3. Mesophase transition entropies of cholesterol alkyl ethers and cholesterol esters of saturated fatty acids (●—●), cholesteric to isotropic transition entropies of ethers; (■—■) smectic to cholesteric transition entropies of ethers; (○---○) cholesteric to isotropic entropies for esters; (□---□) smectic to cholesteric transitions for esters. Data for cholesterol esters are from reference 7.

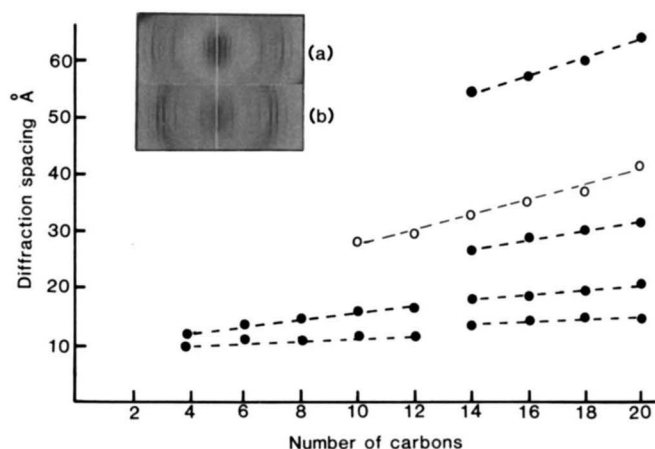


Fig. 4. Primary X-ray diffraction spacing for the crystalline forms of the series of saturated (C_4 – C_{20}) cholesterol alkyl ethers (●—●). The X-ray diffraction patterns in the insert are from a) C_{18} cholesterol ether and b) C_{12} cholesterol ether. Also shown are the diffraction spacings for the single X-ray diffraction observed in the smectic phase for the C_{10} – C_{20} cholesterol ethers (○—○).

gion when examined in the smectic mesophase. This spacing varies linearly with chain length from 26 Å for C_{10} to ~42 Å for C_{20} (Fig. 4).

Cholesterol ethers are uncommon in mammalian tissue; a single study documenting the presence of cholesterol hexadecanoate and octadecanoate ether in bovine heart has been reported (12). However, the structural similarities of cholesterol ethers to cholesterol esters make them ideal for biological studies where probes that do not alter native structural properties are desirable. Our results demonstrate that cholesterol ethers behave thermotropically in a manner analogous to cholesterol esters and in general have stable mesophases in thermodynamic equilibrium over a wider temperature range than the esters. These properties may prove useful in elucidating the structure of cholesterol ether and hence cholesterol ester mesophases. The close structural and thermodynamic similarities of the cholesterol ethers to the esters allows the use of the ethers as nonmetabolizable analogues for cholesterol esters in biological systems such as plasma lipoproteins. **□**

We thank Dr. Y. Stein for stimulating our interest in studying cholesterol ethers. We are grateful to Ms. Eti Butbul for technical assistance and to Dr. Saul Katz, McGill University, Montreal, Canada for the use of his polarizing microscope. This project was supported by the Children's Nutritional Disease Project, Canadian Friends of the Hebrew University, the United States-Israel Binational Science Foundation (no. 1901), and the National Institute of Health (nos. NS02967, HL17675, and NIH26335). Dr. Atkinson is an Established Investigator of the American Heart Association.

Manuscript received 22 September 1982 and in revised form 26 January 1983.

REFERENCES

1. Stein, Y., G. Halperin, and O. Stein. 1981. The fate of cholesteryl linoleyl ether and cholesteryl linoleate in the intact rat after injection of biologically labelled human low density lipoprotein. *Biochim. Biophys. Acta.* **663**: 569–574.
2. Chajek-Shaul, T., G. Friedman, G. Halperin, O. Stein, and Y. Stein. 1981. Uptake of chylomicron [³H]cholesteryl linoleyl ether by mesenchymal rat heart cell culture. *Biochim. Biophys. Acta.* **666**: 147–155.
3. Stein, Y., G. Halperin, and O. Stein. 1980. Biological stability of [³H]cholesteryl oleyl ether in cultured fibroblasts and intact rat. *FEBS Lett.* **111**: 104–106.
4. Halperin, G., and S. Gatt. 1980. The synthesis of cholesteryl alkyl ethers. *Steroids.* **35**: 39–42.
5. Elliot, A. 1965. The use of toroidal reflecting surfaces in X-ray diffraction cameras. *J. Sci. Instrum.* **42**: 312–316.
6. Small, D. M. 1970. The physical state of lipids of biological importance: cholesterol ester, cholesterol, triglyceride. *In Surface Chemistry of Biological Systems.* Plenum Press, New York. 55–83.
7. Davis, G. J., R. S. Porter, and E. M. Barrall II. 1970. An intercomparison of temperatures and heat of transition for esters of cholesterol. *Mol. Cryst. Liq. Cryst.* **11**: 319–330.
8. Craven, B. M., and G. T. DeTitta. 1976. Cholesteryl myristate: structures of the crystalline solids and mesophases. *J. Chem. Soc. Perkin II.* 814.
9. Sawzik, P., and B. M. Craven. 1979. The crystal structure of cholesteryl laurate. *Acta Cryst.* **B35**: 789–791.
10. Craven, B. M., and N. G. Guerina. 1979. The crystal structure of cholesteryl octanoate. *Chem. Phys. Lipids.* **24**: 157–166.
11. Craven, B. M., and N. G. Guerina. 1979. The crystal structure of cholesteryl oleate. *Chem. Phys. Lipids.* **24**: 91–98.
12. Funaski, H., and J. R. Gilbertson. 1968. Isolation and identification of cholesteryl alkyl ethers from bovine cardiac muscle. *J. Lipid Res.* **9**: 766–768.